

Synthesis and characterization of heteroleptic iron(II) thiolate complexes with weak iron–arene interactions

Shun Ohta, Yasuhiro Ohki, Yohei Ikagawa, Rie Suizu, Kazuyuki Tatsumi *

*Department of Chemistry, Graduate School of Science and Research Center for Materials Science, Nagoya University,
Furo-cho, Chikusa-ku, Nagoya 464-8602, Japan*

Received 12 May 2007; received in revised form 19 June 2007; accepted 19 June 2007
Available online 24 June 2007

Dedicated to Professor Gerhard Erker, my friend, on the occasion of his 60th birthday.

Abstract

Selective preparation and characterization of a series of heteroleptic thiolate complexes of iron(II) are described. The compounds were synthesized by treatment of iron bis-amide $\text{Fe}\{\text{N}(\text{SiMe}_3)_2\}_2$ (**1**) with 1 equiv. of terphenyl thiols $\text{HS}(2,6\text{-aryl})_2\text{C}_6\text{H}_3$ followed by addition of another equivalent of different thiol. An amide–thiolate intermediate $[(\text{Me}_3\text{Si})_2\text{N}\{\text{Fe}\}_2(\mu\text{-SDpp})_2$ (**2**; Dpp = 2,6- $\text{Ph}_2\text{C}_6\text{H}_3$) was isolated from the 1:1 reaction of **1** and HSDpp. The X-ray crystal structures of all new thiolate complexes have been determined. The compounds crystallize as monomers or dimers, dependent on the substituents. They consist of distorted tetrahedral or trigonal-planar iron centers with weak interactions between the aromatic rings of thiolate ligands, where the Fe–C(arene) contact is 2.272(2) Å at shortest. The stronger iron–arene interaction appears to induce more pyramidalized geometry at the iron center.
© 2007 Elsevier B.V. All rights reserved.

Keywords: Iron; Thiolate; Heteroleptic complexes; Iron–arene interaction; Terphenyl group; Experimental methods

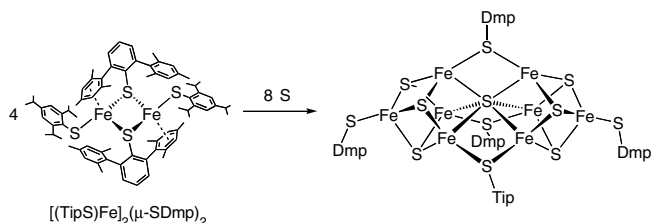
1. Introduction

Synthetic studies on iron thiolate complexes initiated in mid 1970s in relation to the rubredoxin (Rd) center. The model compounds, in which oxidation state is Fe^{II} in $[\text{Fe}(\text{SR})_4]^{2-}$ or Fe^{III} in $[\text{Fe}(\text{SR})_4]^-$, have been prepared and their structures and spectroscopic properties have been compared with those for Rd to provide useful insights [1]. Later, they became also valuable as the precursors for a number of iron–sulfur clusters. Preparations of $[2\text{Fe}-2\text{S}]$, $[3\text{Fe}-4\text{S}]$, $[4\text{Fe}-4\text{S}]$, and $[6\text{Fe}-6\text{S}]$ clusters have been accomplished by treatment of iron–thiolate complexes with elemental sulfur [1a,2]. Notably, iron–thiolates used for cluster synthesis have been mostly limited to anionic and homoleptic compounds $[\text{Fe}(\text{SR})_4]^{2-}$, and the common pathway to produce them is the reaction between iron chlo-

ride and thiolate anions in polar solvents [1]. In such an ion-exchange reaction, as many thiolates as possible attach to the iron center and it generally ends up with tetrakis-thiolate dianions. On the other hand, an acid–base reaction between iron–amide complex $\text{Fe}\{\text{N}(\text{SiMe}_3)_2\}_2$ [3] and thiols in non-polar solvents produces non-ionic compounds and limits the number of thiolate ligands incorporated. This method also appears to be suitable for the preparation of heteroleptic thiolate complexes, as demonstrated for the synthesis of $\text{Fe}_3\{\text{N}(\text{SiMe}_3)_2\}_2(\mu\text{-STip})_4$ (Tip = 2,4,6- $\text{Pr}_3\text{-C}_6\text{H}_2$) [4]. The importance of heteroleptic thiolate complexes is in their potential as precursors for unprecedented types of iron–sulfur clusters, which are relevant to the metal centers in proteins. We have previously succeeded to reproduce the $[8\text{Fe}-7\text{S}]$ core of nitrogenase P-cluster from the reaction of a heteroleptic amide–thiolate complex $\text{Fe}_3\{\text{N}(\text{SiMe}_3)_2\}_2(\mu\text{-STip})_4$ with HSTip, elemental sulfur, and tetramethylthiourea [5]. More recently, a heteroleptic iron–thiolate complex $[(\text{TipS})\text{Fe}]_2(\mu\text{-SDmp})_2$ (Dmp = 2,6-(mesityl) $_2\text{C}_6\text{H}_3$) appeared to serve as a suitable

* Corresponding author.

E-mail address: i45100a@nucc.cc.nagoya-u.ac.jp (K. Tatsumi).



Scheme 1.

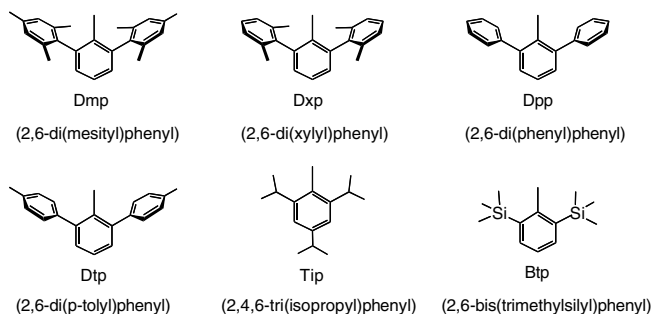


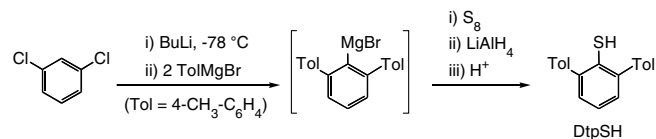
Chart 1. Bulky aryl substituents used in this study.

precursor for an [8Fe–7S] cluster, $[\text{Fe}_8\text{S}_7(\text{SDmp})_2](\mu\text{-SDmp})_2(\mu\text{-STip})$, the structure of which is topologically similar to the FeMo-cofactor of nitrogenase (Scheme 1) [6]. Since its formation is simply achieved by addition of elemental sulfur to a solution of thiolate complex $[(\text{TipS})\text{-Fe}]_2(\mu\text{-SDmp})_2$, variety of thiolate in the precursor likely makes an influence on the structure of resultant iron–sulfur clusters. While some relevant homoleptic thiolate complexes have been reported with bulky thiolates [7,8], we examined the selective preparation of a series of heteroleptic thiolate complexes of iron. Some of bulky thiolates used in this study are able to weakly coordinate to the metal center with their *ortho*-aryl substituents (Chart 1), and stabilize the products as monomeric or dimeric forms.

2. Results and discussion

2.1. Synthesis of *ortho*-substituted thiols

Iron(II) thiolate complexes with a general formulae $\{\text{Fe}(\text{SR})_2\}_n$ readily become polymeric ($n \sim \infty$) via formation of sulfur bridges between iron centers that satisfy the tetrahedral coordination of each iron center. Since the formation of coordination polymers hampers the subsequent use in reactions, this needs to be avoided to maintain homogeneous conditions in organic solvents. An effective way to retard the bridging mode of thiolates is to incorporate a bulky substituent on the sulfur atom. For instance, a bulky SDmp thiolate has been shown to stabilize low-coordinate organometallic and inorganic compounds as monomeric forms [7], and more bulky SAr^* ($\text{Ar}^* = 2,6-(2,4,6\text{-}i\text{-Pr}_3\text{C}_6\text{H}_2)_2\text{C}_6\text{H}_3$) is able to produce a series of divalent, quasi-two-coordinate complexes



Scheme 2.

$\text{M}(\text{SAr}^*)_2$ ($\text{M} = \text{Cr}, \text{Mn}, \text{Fe}, \text{Co}, \text{Ni}, \text{Zn}$) [8]. In this regard, various *ortho*-substituted aryl thiols were used to provide a certain steric bulk around the sulfur atom. One of bulky thiols in this study, DtpSH ($\text{Dtp} = 2,6-(4\text{-CH}_3\text{C}_6\text{H}_4)_2\text{C}_6\text{H}_3$), was prepared by lithiation of 1,3-dichlorobenzene with *n*-BuLi and the subsequent addition of *p*-tolyl Grignard reagents to generate 1-MgBr-2,6-(*p*-tolyl)₂-benzene, followed by treatment with elemental sulfur (Scheme 2). The method to generate terphenyl anion from 1,3-dichlorobenzene has been established by Saednya and Hart [9].

2.2. Synthesis of Fe(II)thiolate complexes

Acid–base reactions between an iron–amide complex $\text{Fe}\{\text{N}(\text{SiMe}_3)_2\}_2$ (**1**) and various bulky thiols were attempted, since an amide ligand on iron is known to serve as a base to deprotonate from added thiols. An important step to accomplish the formation of heteroleptic thiolate complexes is the selective generation of mono-thiolate species of iron, which is denoted as $[(\text{Me}_3\text{Si})_2\text{N}\text{Fe}(\text{SR})]_n$ or its solvent adducts. As reported by Power and co-workers, the reaction of **1** with one equiv of DmpSH produces monomeric $\{(\text{Me}_3\text{Si})_2\text{N}\text{Fe}(\text{SDmp})\}$ [7a]. We and Henkel et al. have also demonstrated that the reactions of **1** with one equiv of $\text{HS}(\text{SiPh}_3)$ or HSBtp ($\text{Btp} = 2,6\text{-bis}(\text{trimethylsilyl})\text{phenyl}$) give rise to dinuclear thiolate complexes $[(\text{Me}_3\text{Si})_2\text{N}\text{Fe}(\text{SAr})]_2(\mu\text{-SR})_2$ ($\text{R} = \text{SiPh}_3$ or Btp) [10]. In a similar manner, relevant reactions with bulky thiols DxpSH ($\text{Dxp} = 2,6-(2,6\text{-Me}_2\text{C}_6\text{H}_3)_2\text{C}_6\text{H}_3$) [11], DppSH ($\text{Dpp} = 2,6\text{-Ph}_2\text{C}_6\text{H}_3$) [12], and DtpSH are expected to produce $[(\text{Me}_3\text{Si})_2\text{N}\text{Fe}(\text{SAr})]_n$ ($n = 1$ or 2). Indeed, a dimeric compound $[(\text{Me}_3\text{Si})_2\text{N}\text{Fe}]_2(\mu\text{-SDpp})_2$ (**2**) was isolated in 70% yield from the 1:1 reaction between **1** and HSDpp . Assuming that similar mono-thiolate complexes are generated in the reactions with DxpSH and DtpSH, another equivalent of different thiol was added to the 1:1 mixture of **1** and these thiols. As summarized in Scheme 3 and Table 1, five heteroleptic thiolate complexes **3–7** were synthesized according to this pathway. Additionally, three new homoleptic thiolate complexes **8–10** were also prepared by addition of 2 equiv. of bulky thiols to **1**. These reactions smoothly underwent and provided the products in high yields as crystals under mild conditions. All compounds are sensitive to air and moisture and need to be handled under inert conditions, while they are thermally stable even after several days in boiling toluene.

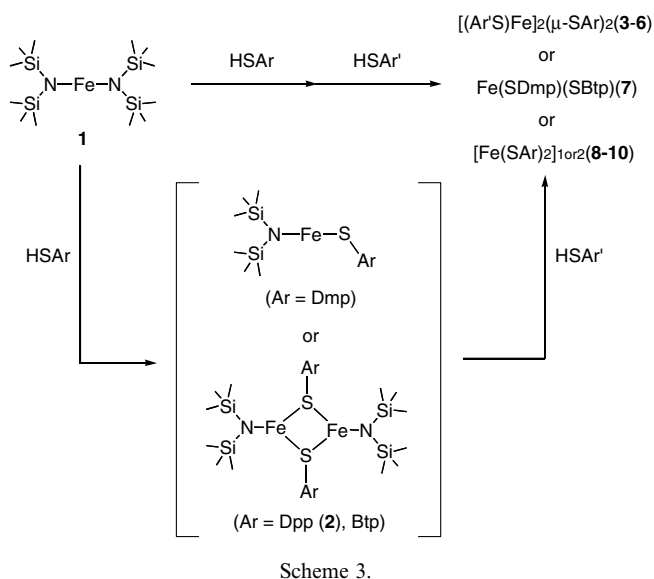


Table 1
Substituents and yields of complexes 3–10

	3	4	5	6	7	8	9	10
Ar	Dpp	Dpp	Dtp	Dxp	Dmp	Dpp	Dtp	Dxp
Ar'	Btp	Tip	Tip	Tip	Btp	Dpp	Dtp	Dxp
Yield	85	94	62	89	56	75	89	95

2.3. X-ray crystal structures of Fe(II) thiolate complexes

All new thiolate complexes 2–10 have been identified by means of X-ray crystallography. The structures of 2–6 and 8–9 are dimeric, whereas 7 and 10 are monomers. Selected bond distances and angles are given in Table 2. Molecular structures of representative complexes 2, 5, 7, and 10 are shown in Figs. 1–4. The structures of dimeric complexes 2–6 and 8 have a crystallographically required center of symmetry at the midpoint between two iron centers. Thus the Fe_2S_2 rings in these complexes are planar and there are two independent $\text{Fe}-\text{S}_{\text{bridge}}$ distances. Whereas complex 9 was analyzed as an entire molecule without symmetric center between iron atoms, the Fe_2S_2 ring is planar with torsion $\text{S}(1)-\text{Fe}(1)-\text{Fe}(2)-\text{S}(2)$ angle of $178.89(9)^\circ$ and the bond distances and angles around two iron centers are

Table 2
Selected data for $[(\text{Me}_3\text{Si}_2\text{N})\text{Fe}]_2(\mu\text{-SDpp})$ (2) and $[\text{Fe}(\text{SAr})(\text{SAr}')_n]$, (3–10, $n = 1$ or 2)

Compound	Ar	Ar'	Yield (%)	Fe–C(arene)	Fe–S–Fe	($\mu\text{-S}$)–Fe–($\mu\text{-S}$)	Fe– S_{bridge}	Fe– $\text{S}_{\text{terminal}}$	Fe–Fe
2	Dpp	–	70	2.589(2)	84.342(15)	95.658(19)	2.3790(6), 2.4013(4)	–	3.2093(4)
3	Dpp	Btp	85	2.579(2)	80.37(2)	99.63(2)	2.3404(10), 2.3689(7)	2.2851(8)	3.0389(6)
4	Dpp	Tip	94	2.341(3)	79.39(3)	100.61(3)	2.3682(10), 2.3631(11)	2.2593(10)	3.0218(8)
5	Dtp	Tip	62	2.272(2)	76.09(2)	103.91(2)	2.3498(6), 2.3698(6)	2.2504(6)	2.9086(4)
6	Dxp	Tip	89	2.438(4)	80.38(3)	99.62(3)	2.3749(10), 2.3898(10)	2.2730(12)	3.0747(7)
7	Dmp	Btp	56	2.389(2)	–	–	–	2.2782(7), 2.2497(6)	–
8	Dpp	Dpp	75	2.417(3)	78.13(2)	101.87(2)	2.3396(7), 2.3686(6)	2.2794(6)	2.9673(5)
9	Dtp	Dtp	89	2.335(9)	77.49(10)	102.60(11)	2.364(2), 2.378(2)	2.265(2), 2.268(3)	2.966(2)
10	Dxp	Dxp	95	2.315(9)	77.36(9)	102.54(11)	2.376(3), 2.368(2)	–	–
				2.437(4)	–	–	–	2.2497(9), 2.2905(13)	–

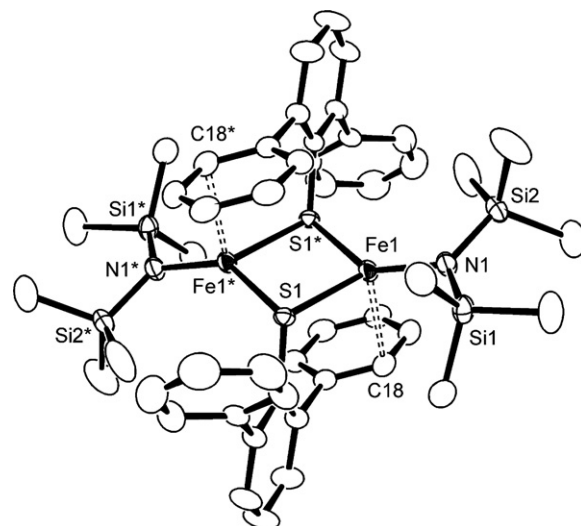


Fig. 1. Molecular structure of $[(\text{Me}_3\text{Si}_2\text{N})\text{Fe}]_2(\mu\text{-SDpp})_2$ (2), showing 50% probability ellipsoids. Hydrogen atoms are omitted for clarity.

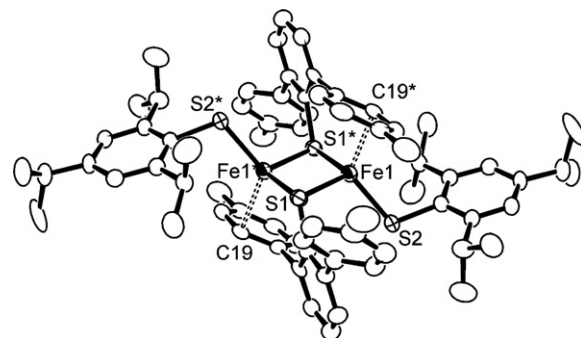


Fig. 2. Molecular structure of $[(\text{TipS})\text{Fe}]_2(\mu\text{-SDtp})_2$ (5), showing 50% probability ellipsoids. Hydrogen atoms are omitted for clarity.

almost identical. As expected, the $\text{Fe}-\text{S}_{\text{bridge}}$ bond lengths are significantly longer than the $\text{Fe}-\text{S}_{\text{terminal}}$ distances. The $\text{Fe}-\text{Fe}$ distances which vary between 2.9086(4) and 3.2093(4) Å are indicative of no direct $\text{Fe}-\text{Fe}$ interaction, although the $\text{Fe}-\text{S}-\text{Fe}$ angles are acute ($76.09(2)$ – $84.342(15)^\circ$). The substituents on bridging sulfur atoms are mutually *trans* to each other with respect to the Fe_2S_2 ring. It is notable that terphenyl thiolates occupy the bridging positions, and one of aryl substituents in the bridging

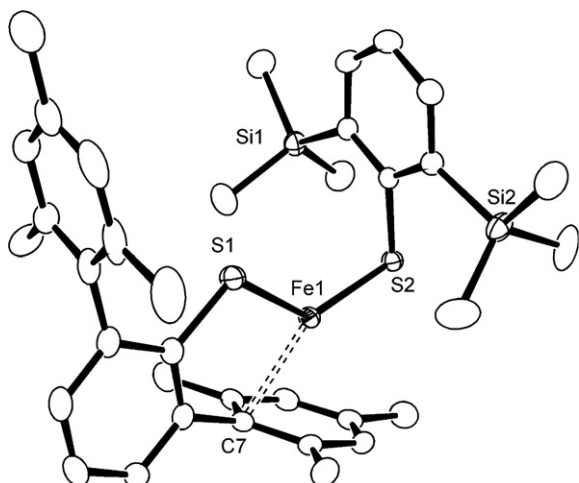


Fig. 3. Molecular structure of Fe(SDmp)(SBtp) (**7**), showing 50% probability ellipsoids. Hydrogen atoms are omitted for clarity.

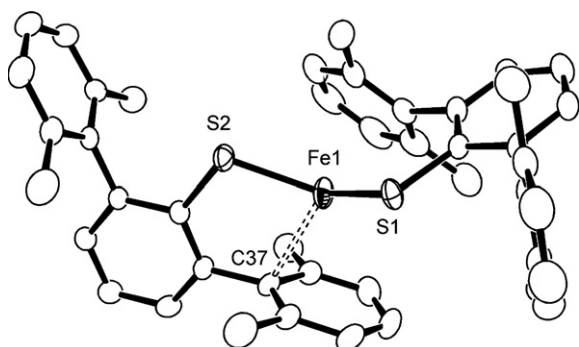


Fig. 4. Molecular structure of Fe(SDxp)₂ (**10**), showing 50% probability ellipsoids. Hydrogen atoms are omitted for clarity.

thiolate ligands is oriented toward the vacant site of each iron center. The weak iron–arene interaction is also indicated by the slightly pyramidalized geometry of iron centers, with the sum of S–Fe–S angles in the range of 330.4–335.0° for **4–6** and **8–9** that exhibit close contact between arene and iron (<2.5 Å). This supplementary Fe–C(arene) interaction efficiently stabilizes the dimeric form of thiolate complexes, with varying the degrees of interaction. The strongest interaction can be seen in **5** where the Fe–C(arene) distance is as short as 2.272(2) Å (Fe–C(19)). This is slightly longer than those in iron–arene compounds (1.92–2.27 Å) in which iron center interacts with η^2 – η^6 π -systems [13]. The Fe–C(arene) distances appeared to be correlated to the (μ -S)–Fe–(μ -S) angles, since stronger Fe–C(arene) interaction leads to more pyramidalized geometry at the iron center that requires wider (μ -S)–Fe–(μ -S) angles.

In contrast to dimers, both compounds **7** and **10** are stabilized as monomers, which is due to larger steric requirements of the bulky substituents. The differences between **7** and **10** are the *ortho*-substituents in one of thiolates, which are SiMe₃ in **7** and xylyl in **10**. The structural features observed in **7** and **10** are common, and both iron centers

interact with one of the *ortho*-aryl groups where the Fe–C(arene) distances are 2.389(2) (**7**) and 2.437(4) (**10**) Å. Similar Fe–C(arene) interactions are found in relevant monomeric complexes Fe(SDmp)₂ (2.470(3), 2.535(3) Å) and {(Me₃Si)₂N}Fe(SDmp) (2.422–2.459 Å) [7a]. The Fe–S bond lengths are 2.2782(7) and 2.2497(6) Å (**7**) and 2.2497(9) and 2.2905(13) Å (**10**), which are comparable to those observed in Fe(SDmp)₂ (2.275(2) and 2.277(2) Å).

2.4. Properties

The iron–thiolate complexes **2–10** are paramagnetic and their ¹H NMR spectra exhibited dramatically shifted signals from the diamagnetic values for free thiols. For instance, five signals for the Dpp group in **2** were observed at δ 8.8, 0.3, –2.6, –9.9, and –15.8, while the SiMe₃ resonance appeared at δ 16.6. Whereas satisfactory assignments for complexes **3–8** were not successful, the complexity of the NMR spectra of **4–6** and **8** indicated that the dimeric framework is retained in solution. Interestingly, the ¹H NMR spectrum of **10** shows equivalent Dxp groups, indicating the reversible coordination of xylyl groups to iron on the NMR time scale.

In the light of paramagnetic nature of **2–10**, the magnetic moments in solution were determined by the Evans method [14]. The monomeric complexes **7** and **10** afforded magnetic moments 5.3 and 5.1 μ_B , respectively, which are consistent with four unpaired electrons and a quintet ground state for d⁶ high-spin configuration (spin only value: 4.89 μ_B). The magnetic moments for dimeric complexes **2–6**, **8**, and **9** are lower and between 2.3 and 4.6 μ_B , owing to antiferromagnetic coupling between the metal centers. The UV–Vis spectra of the iron–thiolate complexes are almost featureless, and their major characteristic is a gradual rise in absorption toward the higher energy region of the spectrum.

3. Conclusion

The use of *ortho*-aryl thiols in acid–base reactions with Fe{N(SiMe₃)₂}₂ appeared to generate iron amide–thiolate species [{(Me₃Si)₂N}Fe(SAr)]_n (*n* = 1 or 2), and the subsequent treatment with different thiols allowed the selective synthesis of a series of heteroleptic thiolate complexes. The bulky substituents efficiently stabilize the compounds as monomers or dimers with weak Fe–arene interactions, which in turn make the compounds highly soluble in organic solvents. While the iron centers are covered by bulky thiolate ligands, the compounds are air-sensitive and highly reactive. This feature would be useful for further reactions with elemental sulfur, donor molecules, and protic reagents.

4. Experimental

All manipulations were carried out under nitrogen atmosphere using standard Schlenk techniques and glove

boxes. THF, hexane, and toluene were purified by the method of Grubbs, where the solvents were passed over columns of activated alumina and supported copper catalyst supplied by Hansen & Co. Ltd. Degassed and distilled solvents from sodium benzophenone ketyl (hexane and toluene) were also used. ^1H NMR (600 MHz) and $^{13}\text{C}\{^1\text{H}\}$ NMR (151 MHz) were recorded on a JEOL ECA600 spectrometer. ^1H NMR chemical shifts are given in ppm relative to the residual protons of deuterated solvents. $^{13}\text{C}\{^1\text{H}\}$ NMR chemical shifts are referenced to signals of C_6D_6 . UV–Vis spectra were measured on a JASCO V560 spectrometer. Elemental analyses were performed on a LECO CHNS-932 micro-analyzer where the samples were sealed into silver capsules in a glovebox. FAB mass spectra were obtained on a JEOL JMS-LCMATE mass spectrometer under a stream of high energy Xe gas, where *m*-nitrobenzyl alcohol was used as the matrix. Iron(II) bis-amide $\text{Fe}\{\text{N}(\text{SiMe}_3)_2\}_2$ [3], DmpSH [7a], DxpSH [11], DppSH [12], BtpSH [15], and TipSH [16] were prepared according to the literature procedures. Other chemicals were used as received.

4.1. Synthesis of 2,6-di-*p*-tolylbenzenethiol (DtpSH)

A hexane solution of *n*-BuLi (1.56 M, 45.0 mL, 70.2 mmol) was added dropwise from a dropping funnel to a solution of 1,3-dichlorobenzene (10.3 g, 70.1 mmol) in THF (200 mL) at -78°C over a period of 10 min, and the reaction mixture was stirred for 1.5 h at -78°C . To the resulting white slurry was slowly added a THF solution of *p*-tolylmagnesium bromide (1.0 M, 147 mL, 147 mmol) from a dropping funnel at -78°C over a period of 30 min. After 1 h, the mixture was allowed to warm to room temperature and refluxed for 2 h. It was cooled in an ice bath and elemental sulfur (11.2 g, 350 mmol) was added to it under positive pressure of nitrogen. The mixture was allowed to warm to room temperature and stirred for 3 h. LiAlH_4 (8.0 g, 210 mmol) was added to it little by little at 0°C and the mixture was stirred overnight at room temperature. The resulting gray slurry was quenched with dilute HCl at 0°C . After removal of THF under reduced pressure, the aqueous mixture was extracted with CH_2Cl_2 (300 mL \times 4) and the organic layer was dried over MgSO_4 . The solvent was removed in vacuo and crystallization of the residue from hot ethyl acetate gave DtpSH (13.5 g, 46.5 mmol, 66%) as colorless crystals. ^1H NMR (600 MHz, C_6D_6): δ 7.32 (d, $J_{\text{H-H}} = 7.9$ Hz, 4H, *o*- or *m*-CH of *p*-tol), 7.13 (d, $J_{\text{H-H}} = 7.6$ Hz, 2H, *m*-CH of Dtp), 6.98 (d, $J_{\text{H-H}} = 7.9$ Hz, 4H, *o*- or *m*-CH of *p*-tol), 6.97 (t, $J_{\text{H-H}} = 7.6$ Hz, 1H, *p*-CH of Dtp), 3.62 (s, 1H, SH), 2.10 (s, 6H, *p*-CH₃ of *p*-tol). $^{13}\text{C}\{^1\text{H}\}$ NMR (151 MHz, C_6D_6): δ 141.4, 139.3, 137.4, 131.9, 129.8, 129.7, 129.6, 124.7, 21.2. FAB-MS (*m*-NBA, Xe): 290 (M^+ , 100). Anal. Calc. for $\text{C}_{20}\text{H}_{18}\text{S}$: C, 82.71; H, 6.25; S, 11.04. Found: C, 82.23; H, 5.94; S, 10.61%.

4.2. Synthesis of $[\{(\text{Me}_3\text{Si})_2\text{N}\}\text{Fe}]_2(\mu\text{-SDpp})_2$ (2)

To a solution of $\text{Fe}\{\text{N}(\text{SiMe}_3)_2\}_2$ (0.500 g, 1.33 mmol) in 15 mL of toluene was added a solution of DppSH (0.348 g, 1.33 mmol) in 15 mL of toluene. The reaction mixture was left stirring for 2 h and then evaporated. The residue was extracted with toluene (5 mL) and centrifuged. The solution was layered with hexane (20 mL) to afford $[\{(\text{Me}_3\text{Si})_2\text{N}\}\text{Fe}]_2(\mu\text{-SDpp})_2$ (2) (0.444 g, 0.465 mmol, 70%) as yellow crystals. ^1H NMR (600 MHz, C_6D_6): δ 16.6 (SiMe₃), 8.8 (Dpp), 0.3 (Dpp), -2.6 (Dpp), -9.9 (Dpp), -15.8 (Dpp). UV–Vis (cyclohexane, λ_{max} , nm (ϵ , $\text{M}^{-1}\text{cm}^{-1}$): 347 (1600), 298 (sh, 5100). Anal. Calc. for $\text{C}_{48}\text{H}_{62}\text{N}_2\text{Fe}_2\text{S}_2\text{Si}_4$: C, 60.36; H, 6.54; N, 2.93; S, 6.71. Found: C, 59.90; H, 6.05; N, 2.85; S, 6.72%. μ_{eff} (Evans method, 296 K): 4.6 μ_{B} .

4.3. Synthesis of $[(\text{BtpS})\text{Fe}]_2(\mu\text{-SDpp})_2$ (3)

To a solution of $\text{Fe}\{\text{N}(\text{SiMe}_3)_2\}_2$ (1.00 g, 2.66 mmol) in 20 mL of toluene was added a solution of DppSH (0.697 g, 2.66 mmol) in 20 mL of toluene, followed by dropwise addition of a solution of BtpSH (0.677 g, 2.66 mmol) in 20 mL of toluene. After 2 h, the solution was concentrated under reduced pressure to ca. 10 mL. An orange powder formed was collected on a frit. Crystallization from toluene at -20°C yielded 3 (1.29 g, 85%) as orange crystals. ^1H NMR (600 MHz, C_6D_6): major signals appeared at δ 17.1, 15.9, 3.3 (SiMe₃), 2.5, -4.1 , -5.7 . UV–Vis (cyclohexane, λ_{max} , nm (ϵ , $\text{M}^{-1}\text{cm}^{-1}$): 427 (2100), 298 (sh, 4600). Anal. Calc. for $\text{C}_{60}\text{H}_{68}\text{Fe}_2\text{S}_4\text{Si}_4$: C, 63.01; H, 6.00; S, 11.02. Found: C, 63.13; H, 6.00; S, 11.24%. μ_{eff} (Evans method, 296 K): 3.5 μ_{B} .

4.4. Synthesis of $[(\text{TipS})\text{Fe}]_2(\mu\text{-SDpp})_2$ (4)

Complex 4 was prepared from $\text{Fe}\{\text{N}(\text{SiMe}_3)_2\}_2$ (1.00 g, 2.66 mmol), DppSH (0.697 g, 2.66 mmol), and TipSH (0.628 g, 2.66 mmol) in a similar manner to that used for 3. Crystallization from toluene at -20°C yielded 4 (1.38 g, 1.25 mmol, 94%) as red crystals. ^1H NMR (600 MHz, C_6D_6): major signals appeared at δ 35.0, 18.5, 16.5, 16.1, 15.5, 8.7, 6.2, 5.0, 4.3, 2.2, -6.3 , -12.1 . UV–Vis (cyclohexane, λ_{max} , nm (ϵ , $\text{M}^{-1}\text{cm}^{-1}$): 403 (3300). Anal. Calc. for $\text{C}_{66}\text{H}_{72}\text{Fe}_2\text{S}_4$: C, 71.72; H, 6.57; S, 11.61. Found: C, 71.57; H, 6.67; S, 11.49%. μ_{eff} (Evans method, 294 K): 3.8 μ_{B} .

4.5. Synthesis of $[(\text{TipS})\text{Fe}]_2(\mu\text{-SDtp})_2$ (5)

Complex 5 was prepared from $\text{Fe}\{\text{N}(\text{SiMe}_3)_2\}_2$ (0.520 g, 1.38 mmol), DtpSH (0.400 g, 1.38 mmol), and TipSH (0.330 g, 1.40 mmol) in a similar manner to that used for 3. Crystallization from toluene at -20°C yielded 5 (0.500 g, 0.430 mmol, 62%) as red crystals. ^1H NMR (600 MHz, C_6D_6): major signals appeared at δ 38.0, 17.6, 15.6, 14.8, 7.9, 5.9, 5.4, 5.0, 4.4, 1.8, 1.0, -5.6 , -14.2 . UV–Vis (cyclohexane, λ_{max} , nm (ϵ , $\text{M}^{-1}\text{cm}^{-1}$): 430

(1800). Anal. Calc. for $C_{70}H_{80}Fe_2S_4$: C, 72.40; H, 6.94; S, 11.04. Found: C, 72.67; H, 6.84; S, 10.74%. μ_{eff} (Evans method, 295 K): 2.5 μ_B .

4.6. Synthesis of $[(\text{TipS})\text{Fe}]_2(\mu\text{-SDxp})_2 \cdot C_7H_8(6 \cdot C_7H_8)$

Complex **6** was prepared from $Fe\{N(\text{SiMe}_3)_2\}_2$ (1.00 g, 2.66 mmol), DxpSH (0.846 g, 2.66 mmol), and TipSH (0.628 g, 2.66 mmol) in a similar manner to that used for **3**. Crystallization from toluene at -20°C yielded $6 \cdot C_7H_8$ (1.55 g, 1.18 mmol, 89%) as red crystals. ^1H NMR (600 MHz, C_6D_6): major signals appeared at δ 28.5, 19.2, 16.5, 12.6, 8.8, 7.9, 2.1, -2.0 , -15.9 . UV–Vis (cyclohexane, λ_{max} , nm (ϵ , $M^{-1} \text{cm}^{-1}$)): 333 (430), 283 (sh, 900). Anal. Calc. for $C_{74}H_{88}Fe_2S_4 \cdot C_7H_8$: C, 74.29; H, 7.39; S, 9.79. Found: C, 74.34; H, 7.09; S, 9.71%. μ_{eff} (Evans method, 295 K): 2.4 μ_B .

4.7. Synthesis of $Fe(\text{SDmp})(\text{SBtp})$ (**7**)

Complex **7** was prepared from $Fe\{N(\text{SiMe}_3)_2\}_2$ (1.00 g, 2.66 mmol), DmpSH (0.920 g, 2.66 mmol), and BtpSH (0.676 g, 2.66 mmol) in a similar manner to that used for **3**. Crystallization from hexane at -20°C yielded **7** (0.974 g, 1.49 mmol, 56%) as orange crystals. ^1H NMR (600 MHz, C_6D_6): major signals appeared at δ 56.1, 37.5, 9.8 (SiMe_3), 3.9. UV–Vis (cyclohexane, λ_{max} , nm (ϵ , $M^{-1} \text{cm}^{-1}$)): 287 (sh, 2300). Anal. Calc. for $C_{36}H_{46}FeS_2Si_2$: C, 66.02; H, 7.08; S, 9.79. Found: C, 66.19; H, 7.11; S, 9.63%. μ_{eff} (Evans method, 296 K): 5.3 μ_B .

4.8. Synthesis of $[(\text{DppS})\text{Fe}]_2(\mu\text{-SDpp})_2$ (**8**)

To a solution of $Fe\{N(\text{SiMe}_3)_2\}_2$ (1.00 g, 2.66 mmol) in toluene (20 mL) was added a solution of DppSH (1.39 g, 5.31 mmol) in toluene (40 mL). The reaction mixture gave a red suspension over the course of a few hours. The suspension was concentrated in vacuo to ca. 10 mL. The red powder was collected on a frit and washed with hexane. Crystallization from toluene at -20°C gave **8** (1.15 g, 0.994 mmol, 75%) as red crystals. ^1H NMR (600 MHz, C_6D_6): major signals appeared at δ 37.6, 18.0, 13.9, 4.9, 3.2, -3.2 , -7.0 , -8.6 , -13.2 . UV–Vis (cyclohexane, λ_{max} , nm (ϵ , $M^{-1} \text{cm}^{-1}$)): 423 (3300). Anal. Calc. for $C_{72}H_{52}Fe_2S_4$: C, 74.73; H, 4.53; S, 11.08. Found: C, 74.72; H, 4.51; S, 11.09%. μ_{eff} (Evans method, 295 K): 4.2 μ_B .

4.9. Synthesis of $[(\text{DtpS})\text{Fe}]_2(\mu\text{-SDtp})_2$ (**9**)

To a solution of $Fe\{N(\text{SiMe}_3)_2\}_2$ (2.36 g, 6.27 mmol) in toluene (150 mL) was added a solution of DtpSH (3.65 g, 12.6 mmol) in toluene (20 mL). The reaction mixture gave an orange suspension over the course of a few hours. The solution was decanted, and the orange microcrystals were washed with hexane and dried to give **9** (3.56 g, 2.80 mmol, 89%). ^1H NMR analysis was not successful due to its low solubility in C_6D_6 . UV–Vis (cyclohexane, λ_{max} , nm (ϵ ,

$M^{-1} \text{cm}^{-1}$): 346 (1200). Anal. Calc. for $C_{80}H_{68}Fe_2S_4$: C, 75.70; H, 5.40; S, 10.10. Found: C, 75.43; H, 5.17; S, 10.00%. The magnetic moment of **9** was not measured because of its low solubility.

4.10. Synthesis of $Fe(\text{SDxp})_2$ (**10**)

To a solution of $Fe\{N(\text{SiMe}_3)_2\}_2$ (0.500 g, 1.33 mmol) in toluene (20 mL) was added a solution of DxpSH (0.846 g, 2.66 mmol) in toluene (20 mL). The reaction mixture was left stirring for 2 h and then evaporated in vacuo. The residue was extracted with toluene (5 mL) and centrifuged. The solution was layered with hexane (20 mL) to afford $Fe(\text{SDxp})_2$ (**10**) (0.871 g, 1.26 mmol, 95%) as red crystals. ^1H NMR (600 MHz, C_6D_6): δ 49.2 (24H, $-\text{CH}_3$), 6.7 (4H, *m*- C_6H_3 or *p*-xylyl), -22.2 (8H, *m*-xylyl), -26.1 (2H + 4H, *p*- C_6H_3 and *m*- C_6H_3 or *p*-xylyl). UV–Vis (cyclohexane, λ_{max} , nm (ϵ , $M^{-1} \text{cm}^{-1}$)): 452 (300), 395 (300), 287 (sh, 750). Anal. Calc. for $C_{44}H_{42}FeS_2$: C, 76.50; H, 6.13; S, 9.28. Found: C, 76.57; H, 5.91; S, 9.41%. μ_{eff} (Evans method, 297 K): 5.1 μ_B .

4.11. X-ray structural analysis

Crystallographic data are summarized in Table 3. Crystals of DtpSH and **2–10** were mounted on a loop using oil (CryoLoop, Immersion Oil, Type B or Paraton, Hampton Research Corp.) and set on a Rigaku AFC-8 instrument equipped with a Mercury CCD detector, with a Saturn CCD detector, or on a Rigaku RA-Micro007 with a Saturn CCD detector by using graphite-monochromated $\text{Mo K}\alpha$ radiation ($\lambda = 0.710690 \text{ \AA}$) under a cold nitrogen stream. The frame data were integrated and corrected for absorption with the Rigaku/MS-CrystalClear package. The structures were solved by direct methods and standard difference map techniques, and were refined with full-matrix least-square procedures on F by a Rigaku/MS-CrystalStructure package. Anisotropic refinement was applied to all non-hydrogen atoms except for the disordered groups. Methyl groups bound to Si(2) in **2** and **7**, the *ortho*- i Pr groups of STip ligand in **4** and $6 \cdot C_7H_8$, one of the xylyl groups in $6 \cdot C_7H_8$, and one of the mesityl groups in **7** are disordered over two positions with 50:50 occupancy factors. The *para*- i Pr group of STip ligand in **4** is disordered over two positions with 60:40 occupancy factors. The crystal solvent toluene is disordered in $3 \cdot C_7H_8$ and $6 \cdot C_7H_8$ over two positions with 50:50 occupancy factors. All hydrogen atoms were placed at calculated positions. Additional crystallographic data are given in the Supporting Information.

4.12. Magnetic moments

The magnetic moments in solution were measured by the method originally described by Evans [14]. A reference is used by placing a sealed capillary containing a mixture of C_6D_6 /cyclohexane (90/10 v/v) and dropped into an NMR

Table 3
Crystal data of DripSH and iron–thiolate complexes 2–10

	2	3 · C ₇ H ₈	4	5	6 · C ₇ H ₈	7	8	9	10
Formula	C ₂₀ H ₁₈ S	C ₆₇ H ₆₈ Fe ₂ S ₄ ·Si ₄	C ₆₆ H ₆₆ Fe ₂ S ₄	C ₇₀ H ₈₀ Fe ₂ S ₄	C ₈₁ H ₉₆ Fe ₂ S ₄	C ₃₆ H ₄₆ Fe ₂ S ₄ Si ₂	C ₇₂ H ₅₂ Fe ₂ S ₄	C ₈₀ H ₆₈ Fe ₂ S ₄	C ₄₄ H ₄₂ Fe ₂ S ₂
Formula weight	290.42	1225.55	1099.18	1161.34	1309.58	654.90	1157.14	1269.35	690.78
Crystal system	Monoclinic	Monoclinic	Monoclinic	Monoclinic	Monoclinic	Monoclinic	Monoclinic	Monoclinic	Monoclinic
Space group	P2 ₁ /a (#14)	P2 ₁ /n (#14)	P2 ₁ /c (#14)	P2 ₁ /n (#14)	P2 ₁ /n (#14)	C2/c (#15)	P2 ₁ /a (#14)	Cc (#9)	P2 ₁ (#4)
a (Å)	12.377(2)	14.044(6)	13.705(4)	9.4360(11)	12.2426(13)	26.090(6)	12.367(4)	16.940(4)	8.2225(18)
b (Å)	7.3013(13)	15.324(6)	11.275(3)	27.876(3)	21.419(2)	15.891(4)	19.850(6)	16.305(3)	15.576(3)
c (Å)	17.704(3)	15.665(7)	18.435(5)	11.7967(13)	13.6990(15)	18.246(5)	12.240(4)	23.554(5)	13.972(3)
β (°)	97.825(3)	106.302(6)	100.336(5)	91.0047(16)	93.004(2)	109.077(3)	112.958(4)	105.316(3)	97.746(3)
V (Å ³)	1585.1(5)	3236(2)	2802.3(12)	3102.5(6)	3587.2(7)	7149(3)	2766.8(15)	6275(2)	1773.0(7)
Z	4	2	2	2	2	8	2	4	2
D _{calc} (g cm ⁻³)	1.217	1.258	1.281	1.230	1.175	1.179	1.389	1.336	1.294
μ (cm ⁻¹)	1.950	6.892	7.058	6.412	5.612	6.266	7.200	6.411	5.732
F(000)	616.00	1284.00	1120.00	1208.00	1316.00	2624.00	1200.00	2628.00	728.00
2θ _{max} (°)	55.0	55.0	55.0	55.0	55.0	55.0	55.0	55.0	55.0
Number of reflections collected	12445	25956	22293	24481	28808	41183	21458	24852	14479
Independent reflections	3428	7317	6162	6904	7739	8126	6185	11684	4097
Number of parameters	207	370	345	375	389	384	378	826	466
R ^a	0.0752	0.0635	0.0921	0.0587	0.0922	0.0582	0.0536	0.0690	0.0445
R _w ^b	0.0764	0.0863	0.0982	0.0906	0.1009	0.0876	0.0601	0.0835	0.0696
Goodness-of-fit	1.038	1.172	1.067	1.061	1.167	0.991	1.002	1.204	1.000

^a $R = \sum |F_o| - |F_c| / \sum |F_o|$
^b $R_w = \sum w(|F_o| - |F_c|)^2 / \sum w F_o^2$

tube containing the solution of the complex (~10 mg) in a mixture of C₆D₆/cyclohexane (90/10 v/v). The chemical shift difference of the cyclohexane signal between the inner and the outer tubes was measured. From this difference in the chemical shift the molar susceptibility χ_M and the magnetic moment μ_{eff} can be calculated with Eqs. (1) and (2) (given in S.I. units)

$$\chi_M = \frac{3 \cdot \Delta f}{1000 \cdot f \cdot c} \quad (1)$$

$$\mu_{\text{eff}} = \sqrt{\frac{3k}{N_A \cdot \mu_0 \cdot \mu_B^2} \cdot T \cdot \chi_M} = 798 \sqrt{T \cdot \chi_M} \quad (2)$$

χ_M is the molar susceptibility of the complex in m³ mol, Δf the difference in the chemical shift in Hz, f the frequency of operation of the spectrometer in Hz, c the concentration of the complex in mol dm⁻³, and T is the temperature in K.

Acknowledgements

This research was financially supported by a Grant-in-Aid for Scientific Research (Nos. 18GS0207 and 18064009) from the Ministry of Education, Culture, Sports, Science and Technology, Japan.

Appendix A. Supplementary material

CCDC 643482, 643483, 643484, 643485, 643486, 643487, 643488, 643489, 643490, and 643491 contain the supplementary crystallographic data for this paper. These data can be obtained free of charge via <http://www.ccdc.cam.ac.uk/conts/retrieving.html>, or from the Cambridge Crystallographic Data Centre, 12 Union Road, Cambridge CB2 1EZ, UK; fax: (+44) 1223-336-033; or e-mail: deposit@ccdc.cam.ac.uk. Supplementary data associated with this article can be found, in the online version, at doi:10.1016/j.jorganchem.2007.06.027.

References

- [1] (a) P.V. Rao, R.H. Holm, Chem. Rev. 104 (2004) 527;
 (b) R.H. Holm, Acc. Chem. Res. 10 (1977) 427;
 (c) P.J. Blower, J.R. Dilworth, Coord. Chem. Rev. 76 (1987) 121;
 (d) I.G. Dance, Polyhedron 5 (1986) 1037;
 (e) M.V. Twigg, J. Burgess, in: J.A. McCleverty, T.L. Meyer (Eds.), Comprehensive Coordination Chemistry II, vol. 5, Pergamon, Elsevier, 2004 (Chapter 5.4);
 (f) J. Burgess, M.V. Twigg, in: R.B. King (Ed.), Encyclopedia of Inorganic Chemistry, vol. 4, Wiley, New York, 2005, p. 2250.
- [2] (a) R.H. Holm, in: J.A. McCleverty, T.L. Meyer (Eds.), Comprehensive Coordination Chemistry II, vol. 8, Pergamon, Elsevier, 2004 (Chapter 8.3);
 (b) J.G. Reynolds, R.H. Holm, Inorg. Chem. 19 (1980) 3257;
 (c) K.S. Hagen, J.G. Reynolds, R.H. Holm, J. Am. Chem. Soc. 103 (1981) 4054;
 (d) K.S. Hagen, R.H. Holm, J. Am. Chem. Soc. 104 (1982) 5496;
 (e) P.K. Mascharak, M.C. Smith, W.H. Armstrong, B.K. Burgess, R.H. Holm, Proc. Natl. Acad. Sci. USA 79 (1982) 7056;
 (f) D.W. Stephan, G.C. Papaefthymiou, R.B. Frankel, R.H. Holm, Inorg. Chem. 22 (1983) 1550;

- (g) K.S. Hagen, A.D. Watson, R.H. Holm, *J. Am. Chem. Soc.* 105 (1983) 3905;
- (h) P.K. Mascharak, K.S. Hagen, J.T. Spence, R.H. Holm, *Inorg. Chim. Acta* 80 (1983) 157;
- (i) M.G. Kanatzidis, W.R. Dunham, W.R. Hagen, D. Coucouvanis, *J. Chem. Soc., Chem. Commun.* (1984) 356;
- (j) M.G. Kanatzidis, W.R. Hagen, W.R. Dunham, R.K. Lester, D. Coucouvanis, *J. Am. Chem. Soc.* 107 (1985) 953;
- (k) S. Han, R.S. Czernuszewicz, T.G. Spiro, *Inorg. Chem.* 25 (1986) 2276;
- (l) U. Bierbach, W. Saak, D. Haase, S. Pohl, *Z. Naturforsch., B: Chem. Sci.* 46 (1991) 1629;
- (m) U.-A. Opitz, B. Bahlmann, S. Pohl, *Z. Naturforsch., B: Chem. Sci.* 51 (1996) 1040.
- [3] R.A. Andersen, K. Faegri Jr., J.C. Green, A. Haaland, M.F. Lappert, W.-P. Leung, K. Rypdal, *Inorg. Chem.* 27 (1988) 1782.
- [4] F.M. McDonnell, K. Ruhlandt-Senge, J.J. Ellison, R.H. Holm, P.P. Power, *Inorg. Chem.* 34 (1995) 1815.
- [5] Y. Ohki, Y. Sunada, M. Honda, M. Katada, K. Tatsumi, *J. Am. Chem. Soc.* 125 (2003) 4052.
- [6] Y. Ohki, Y. Ikagawa, K. Tatsumi, *J. Am. Chem. Soc.* 129 (2007) in press.
- [7] (a) J.J. Ellison, K. Ruhlandt-Senge, P.P. Power, *Angew. Chem., Int. Ed. Engl.* 33 (1994) 1178;
- (b) M. Niemeyer, P.P. Power, *Inorg. Chem.* 35 (1996) 7264;
- (c) Y. Ohki, H. Sadohara, Y. Takikawa, K. Tatsumi, *Angew. Chem., Int. Ed. Engl.* 43 (2004) 2290.
- [8] T. Nguyen, A. Panda, M.M. Olmstead, A.F. Richards, M. Stender, M. Brynda, P.P. Power, *J. Am. Chem. Soc.* 127 (2005) 8545.
- [9] A. Saednya, H. Hart, *Synthesis* (1996) 1455.
- [10] (a) R. Hauptmann, R. Klib, J. Schneider, G. Henkel, *Z. Anorg. Allg. Chem.* 624 (1998) 1927;
- (b) T. Komuro, T. Matsuo, H. Kawaguchi, K. Tatsumi, *Inorg. Chem.* 42 (2003) 5340.
- [11] U. Luning, H. Baumgartner, *Synlett* 8 (1993) 571.
- [12] P.T. Bishop, J.R. Dilworth, T. Nicholson, J. Zubieta, *J. Chem. Soc., Dalton Trans.* (1991) 385.
- [13] (a) R.C. Kerber, in: E.W. Abel, F.G.A. Stone, G. Wilkinson (Eds.), *Comprehensive Organometallic Chemistry*, vol. 7, Pergamon, Oxford, 1995 (Chapter 2);
- (b) R.S. Paley, in: R.B. King (Ed.), *Encyclopedia of Inorganic Chemistry*, vol. 4, Wiley, New York, 2005, p. 2307;
- (c) D. Astruc, *Acc. Chem. Res.* 19 (1986) 377;
- (d) D. Astruc, *Chem. Rev.* 88 (1988) 1189;
- (e) D. Astruc, *Acc. Chem. Res.* 30 (1997) 383;
- (f) D. Astruc, *Acc. Chem. Res.* 33 (2000) 287.
- [14] (a) D.F. Evans, *J. Chem. Soc.* (1959) 2003;
- (b) G.J.P. Britovsek, V.C. Gibson, S.K. Spitzmesser, K.P. Tellmann, A.J.P. White, D.J. Williams, *J. Chem. Soc., Dalton Trans.* (2002) 1159.
- [15] E. Block, V. Eswaralrishnan, M. Gernon, G. Ofori-Okai, C. Saha, K. Tang, J. Zubieta, *J. Am. Chem. Soc.* 111 (1989) 658.
- [16] P.J. Blower, J.R. Dilworth, J.P. Hutchinson, J.A. Zubieta, *J. Chem. Soc., Dalton Trans.* (1985) 1533.